BUDOWNICTWO
CZASOPISMO TECHNICZNE
TECHNICAL TRANSACTIONS
CIVIL ENGINEERING
WYDAWNICTWO POLITECHNIKI KRAKOWSKIEJ
1-B/2011
ZESZYT 3
ROK 108
ISSUE 3
YEAR 108

MICHAŁ WCISŁO*

TRAIN AXES SPACING INFLUENCE ON DYNAMICAL BEHAVIOUR OF A GIRDER BRIDGE

WPŁYW ROZSTAWU OSI POCIĄGU NA DYNAMICZNE ZACHOWANIE MOSTU BELKOWEGO

A b s t r a c t

In the paper the influence of moving load spacing to dynamical behavior of an Euler--Bernoulli beam was analyzed. The critical speed problem for forces moving along an elastic beam was defined and introduced. The analysis was carried out for three different mechanical models of load.

Keywords: bridge dynamics, critical speed, load model

S t r e s z c z e n i e

W niniejszym artykule przeprowadzono analizę wpływu rozstawu obciążeń przemieszczających się wzdłuż belki Eulera-Bernoullego na jej zachowanie dynamiczne. Zdefiniowano i przedstawiono pojęcie prędkości krytycznej dla przemieszczającej się siły. Analizę wpływu rozstawu przeprowadzono z uwzględnieniem różnych modeli mechanicznych obciążenia.

Słowa kluczowe: dynamika mostów, prędkość krytyczna, modele obciążeń

* MSc. Eng. Michał Wcisło, Institute of Road and Railway Engineering, Faculty of Civil Engineering, Cracow University of Technology.

1. Introduction

Permanent growth of conventional railway transport speeds causes need for assuring higher stability and smoothness of ride. What is more, the increase of speeds usually results in stronger dynamical effects in behavior of railway track and bridge structures. As a result it is very essential during the design process to take into account as many dynamical problems as possible. In this paper a numerical simulation of influence of load spacing (interpreted as car length) on a bridge structure was carried out.

2. Mechanical model

In this paper a simple, Euler-Bernoulli beam subjected to a series of loads moving with constant speed, is analyzed. In order to research critical speeds (Chapter 4) the load is modeled as a single force (fig. 1a), single mass (fig. 1b), or a single mechanical oscillator (fig. 1c). Further the influence of load spacing on the dynamical behavior of a girder bridge was analyzed. For this reason three following double load models and one triple load model were applied: a double force model (fig. 2a), a rigid body supported in two points model (fig. 2b), a double mechanical oscillator model (fig. 2c), and an equally spacing, triple force model (fig. 2d).

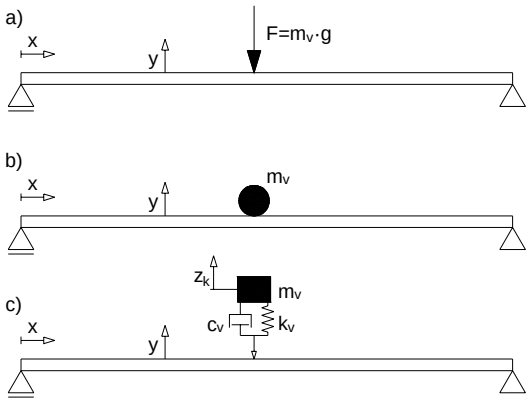

Fig. 1. Critical speeds analysis load models

Rys. 1. Modele obciążeń dla badania prędkości krytycznych

The Euler-Bernoulli simple beam governing equation [3]

$$m(x)\frac{\partial^2 y(x,t)}{\partial t^2} + C_y(x)\frac{\partial y(x,t)}{\partial t} + \frac{\partial^2}{\partial x^2}\left(EI(x)\frac{\partial^2 y(x,t)}{\partial x^2}\right) = P_b(x,t) \tag{1}$$

where:

- $m(x)$ – the beam mass per unit length,
- $y(x, t)$ – the beam deflection,
- $C_y(x)$ – the beam damping,
- $EI(x)$ – the beam bending stiffness,
- $P_b(x, t)$ – load.

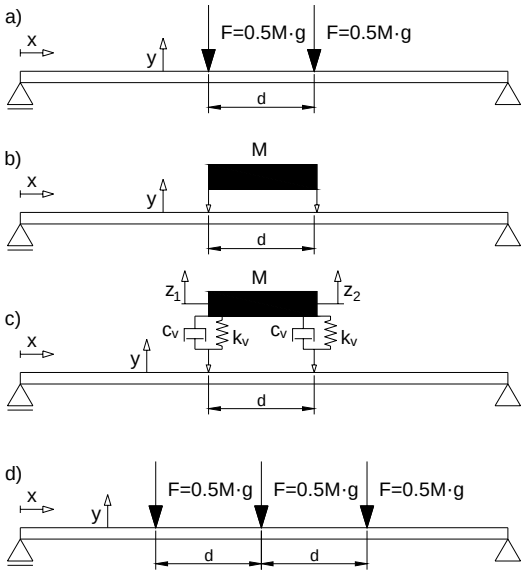

Fig. 2. Loads spacing analysis load models

Rys. 2. Modele obciążeń dla ustalania wpływu ich rozstawu na zachowanie belki

The problem was simplified by assuming constant values of $m(x)$, $C_y(x)$, $EI(x)$, what results in change of the (1) equation to

$$m\frac{\partial^2 y(x,t)}{\partial t^2}+C_y\frac{\partial y(x,t)}{\partial t}+EI(x)\frac{\partial^4 y(x,t)}{\partial x^4}=P_b(x,t) \tag{2}$$

where:

$$P_b(x,t)=-\sum_{k=1}^{N_v}p_k\cdot\delta\left[x-v\cdot\left(t-t_k\right)\right]\cdot H_0\left(t,t_k\right) \tag{3}$$

$$H_0\left(t,t_k\right)=U\left(t-t_k\right)-U\left[t-\left(t_k+\frac{L}{v}\right)\right] \tag{4}$$

$$\delta(x)=\begin{cases}\infty & \text{for } x=0\\ 0 & \text{for } x\neq 0\end{cases} \qquad \text{and} \qquad \int_{-\infty}^{\infty}\delta(x)dx=1 \tag{5}$$

$$U(t)=\begin{cases}1 & \text{for } t\geq 0\\ 0 & \text{for } t<0\end{cases} \tag{6}$$

N_v – number of loads,
t_k – the k load time of approach of the beginning of the bridge,
L – the bridge length,
v – speed of moving load.

Each model differs from others in construction of the p_k term.

2.1. Single force model (fig. 1a)

$$p_k = m_v \cdot g \qquad \text{and} \quad k = 1 \tag{7}$$

where:

m_v – the load mass,
g – gravitational acceleration.

2.2. Single mechanical oscillator model (fig. 1c)

$$p_k = m_v \cdot g + k_v \cdot (y_0 - z) + c_v \cdot (\dot{y}_0 - \dot{z}) = m_v \cdot [g + \ddot{z}(t)] \qquad \text{and} \quad k = 1 \tag{8}$$

where:

z – vertical displacement of the bogie mass,
y_0 – the current beam deflection under the load.

In order to solve this problem an indirect- iterative method was applied. In the first step a force runs along the beam, what results in its deflecting. The acquired deformation history is further taken as the kinematic constraint in the second step, in which the vertical bogie mass movement history is obtained. In the third step the mechanical oscillator with a priori known vertical displacement history interacts with the beam as shown in (8). The second and the third steps compose an iteration, which may be repeated to achieve required accuracy. The iteration convergence is very fast, so for purposes of this paper it was assumed, that one iteration is precise enough to carry out the simulation reliably.

2.3. Single mass model (fig. 1b)

This model is the same as the single mechanical oscillator model, but the bogie stiffness is many times greater.

2.4. Double force model (fig. 2a)

This model is the same as the single force model, but: $k = 1, 2$

2.5. Double mechanical oscillator model (fig. 2c)

To solve this problem an iterative method, analogical to 2.2 was applied, but in this case the kinematic constraint obtained from the first step acts on a rigid mass with two degrees of freedom.

$$p_{ki} = 0.5 \cdot M \cdot g + k_v \cdot (y_k - z_k) + c_v \cdot (\dot{y}_k - \dot{z}_k) \qquad \text{and} \quad k = 1, 2 \tag{9}$$

where:

z_k – vertical displacement of the rigid bogie mass k point,
y_k – current deflection of beam under the k point.

2.6. Rigid body supported in two points model

This model is the same as the double mechanical oscillator model, but bogies stiffness is many times greater.

3. Numerical model

The solution of the governing equation was assumed to be a sum of products of time functions and position functions [2].

$$y(x,t) = \sum_{j=1}^{N} \varphi_j(x) \cdot \eta_j(t) = \Phi^T(x) \cdot \mathrm{H}(t) \tag{10}$$

where:

$\Phi(x)$ – vector of shape functions of first natural modes of the beam,
N – number of natural modes taken into account.

Putting the (10) into (2), multiplying both sides by $\Phi(x)$ and integrating with respect to x variable gives

$$\begin{aligned} &\left(\int_0^L \Phi(x) \cdot m \cdot \Phi^T(x) dx\right) \ddot{\mathrm{H}}(t) + \left(\int_0^L \Phi(x) \cdot C_y \cdot \Phi^T(x) dx\right) \dot{\mathrm{H}}(t) + \left(\int_0^L \Phi(x) \cdot EI \cdot \Phi^T(x)^{\mathrm{IV}} dx\right) \mathrm{H}(t) \\ &= -\sum_{k=1}^{Nv} p_k \cdot \Phi\left[v\left(t - t_k\right)\right] \cdot H_0(t, t_k) \end{aligned} \tag{11}$$

or as matrices

$$\left[M_b\right] \cdot \ddot{\mathrm{H}}(t) + \left[C_b\right] \cdot \dot{\mathrm{H}}(t) + \left[K_b\right] \cdot \mathrm{H}(t) = F_b(t) \tag{12}$$

For a simple beam vector of first natural modes consists of following terms

$$\Phi(x) = \left\{ \sin\frac{\pi \cdot v}{L}, \sin\frac{2\pi \cdot v}{L}, ..., \sin\frac{N\pi \cdot v}{L} \right\} \tag{13}$$

Matrices $[M_b]$, $[C_b]$, $[K_b]$ are diagonal, so the system of equations (12) can be divided into N independent, linear, ordinary differential equations

$$M_{bj} \cdot \ddot{\eta}_j(t) + C_{bj} \cdot \dot{\eta}_j(t) + K_{bj} \cdot \eta_j(t) = F_{bj}(t) \tag{14}$$

with initial conditions

$$\dot{\eta}_j(0) = 0, \qquad \eta_j(0) = 0 \qquad \forall j = 1, 2, ..., N \tag{15}$$

Constant coefficients of these equations can be written as

$$M_{bj} = \int_0^L m \cdot \varphi_j{}^2(x)dz = m \cdot \int_0^L \left(\sin \frac{j \cdot \pi \cdot x}{L} \right)^2 dx = m \cdot \frac{L}{2} \tag{16}$$

$$C_{bj} = \int_0^L C_y \cdot \varphi_j{}^2(x)dx = C_y \cdot \frac{L}{2} \tag{17}$$

$$K_{bj} = \int_0^L \varphi_j(x) \cdot EI \cdot (\varphi_j(x))^{\mathrm{IV}} dx = \frac{EI \cdot (j \cdot \pi)^4}{2 \cdot L^3} \tag{18}$$

$$F_{bj} = -\sum_{k=1}^{N_v} p_k \cdot \varphi_j[v(t - t_k)] \cdot H_0(t, t_k) \tag{19}$$

This problem was solved with the Finite Difference Method (FDM) applied in Python enviroment program. For calculations following parameters were taken:
dt = 0.0002 sec the FDM time step
N = 10
C_y = 0

4. Critical speeds of a load moving along a simple beam

Loads acting on an Euler-Bernoulli beam cause deformations, which depend on the load position history and load value history. If the problem is simplified to only one constant force, moving along the beam with a constant speed, then one can find a particular value of speed, which the beam gets excited extremely for. The value of displacement of the point under the load is further treated as the degree of beam excitement.

A simple beam with following mechanical parameters was analyzed:
EI = 22e10 m^{4}N/m^2
m = 60000 kg/m
L = 40 m

In most cases of dynamical analyses first natural mode is the most important element of dynamical behavior of a mechanical system. In this paper the first mode is the base for determining a particular value of the critical speed. If time, in which the moving force causes increase of deflection of the mid-span equals the time of uninterrupted increase of deflection in the first mode of natural vibration, than the beam gets excited extremely. Consequently- one should expect maximal degree of excitation if total time of passing the beam by the load equals period of the first natural mode, and the speed corresponding with this situation is called the critical speed.

$$v_{\mathrm{kr}} = \frac{L}{T} \tag{20}$$

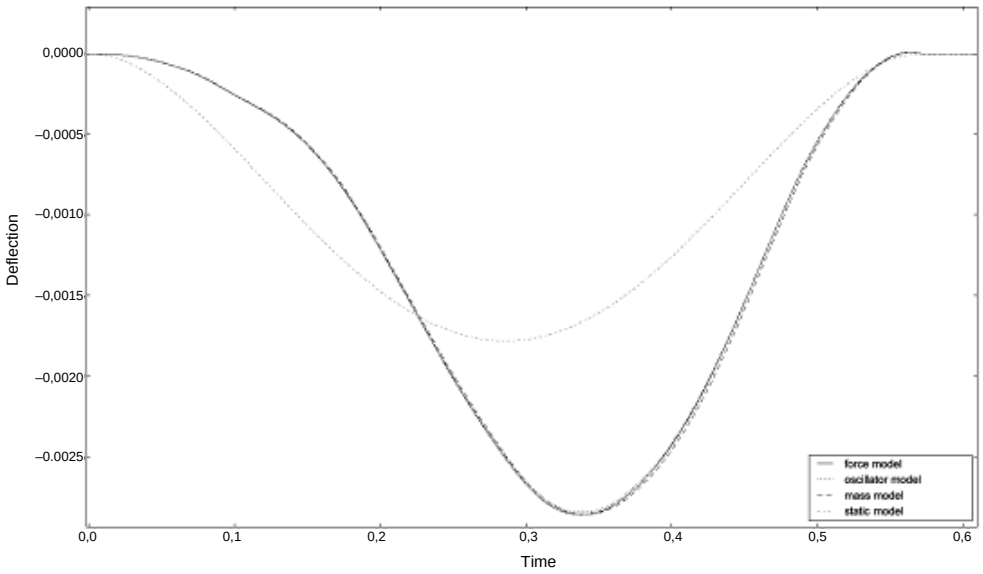

Fig. 3. An example of deflection of the beam under load by v = 70 m/sec

Rys. 3. Przykład ugięcia belki w punkcie pod obciążeniem dla v = 70 m/s

For a simple beam the first mode angular frequency, frequency and period are as follows

$$\omega_1 = \pi^2 \sqrt{\frac{EI}{m \cdot L^4}} = 11.812 \text{ rad/sec} \tag{21}$$

$$f_1 = \frac{\omega_1}{2 \cdot \pi} = 1.8799 \text{ Hz} \tag{22}$$

$$T_1 = \frac{1}{f_1} = 0.5319 \text{ sec} \tag{23}$$

And finally – the critical speed

$$v_{kr} = 75.20 \frac{\text{m}}{\text{sec}} = 270.7 \frac{\text{km}}{\text{h}} \tag{24}$$

The above consideration was verified by a numerical analysis. The beam was exposed to loads moving with different speeds. All three models mentioned in the Chapter 2 were applied, and the mass value was set to 30000 kg.

Table 1 shows results for different values of speeds, and for each of them a maximal value of deflection and maximum deflection relative location. Although only first natural mode was taken into account, the simulation results correspond with expected value of critical speed, what may prove that this method is reliable.

Table 1

Comparison of numerical simulation results

Speed [m/sec]	Force model		Oscillator model		Mass model	
	u_{max} [mm]	x_{max}/L	u_{max} [mm]	x_{max}/L	u_{max} [mm]	x_{max}/L
50	2,66	0,499	2,65	0,499	2,67	0,504
60	2,83	0,552	2,82	0,552	2,84	0,557
70	2,86	0,592	2,85	0,590	2,86	0,595
80	2,81	0,626	2,80	0,626	2,81	0,632
90	2,68	0,659	2,67	0,659	2,67	0,664
100	2,49	0,688	2,48	0,688	2,48	0,693

Results

In order to estimate influence of spacing on deflection of the analyzed beam, its behavior was studied in two variants of speeds: 60 m/sec and 70 m/sec, always under the last load. Ratio of maximal deflection and corresponding maximal static deflection (deflection excluding dynamical effects) was treated as the measure of influence of spacing.

The biggest deformations are expected to appear for spacing d_1, causing entering of loads with frequency equal to the first natural mode frequency, while the smallest deformations are expected to appear for spacing d_{opt}, causing entering of loads with frequency twice as big, so even loads would excite the beam inversely to odd loads.

4.1. Results for speed v = 60 m/sec

d_1 = 31.92 m
d_{opt} = 15.96 m

4.1.1. Double loading

Table 2

Deflection under the second load for v = 60 m/sec

Spacing [m]	Force model			Oscillator model			Rigid mass model			Static deflection u_{stat} [m]
	u_{max} [mm]	x_{max}/L	u_{max}/u_{stat}	u_{max} [mm]	x_{max}/L	u_{max}/u_{stat}	u_{max} [mm]	x_{max}/L	u_{max}/u_{stat}	
9	4,81	0,470	1,508	4,78	0,470	1,498	4,87	0,476	1,527	3,19
12	4,12	0,438	1,401	4,10	0,440	1,395	4,18	0,446	1,422	2,94
15	3,32	0,395	1,248	3,31	0,396	1,244	3,37	0,399	1,267	2,66
18	2,48	0,363	1,055	2,49	0,366	1,060	2,53	0,368	1,077	2,35
21	1,74	0,474	0,861	1,76	0,474	0,871	1,75	0,468	0,866	2,02
24	2,06	0,651	1,157	2,05	0,648	1,152	2,03	0,653	1,140	1,78
27	2,67	0,647	1,500	2,64	0,647	1,483	2,65	0,651	1,489	1,78
30	3,24	0,627	1,820	3,21	0,627	1,803	3,24	0,632	1,820	1,78

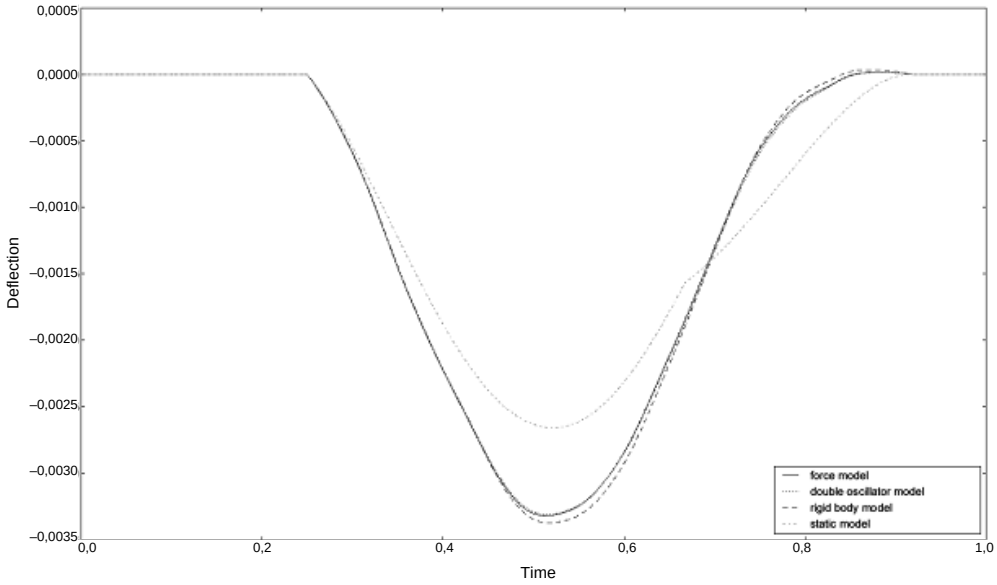

Fig. 4. An example of deflection of the beam under the second load by d = 15 m

Rys. 4. Przykład ugięcia belki w punkcie pod drugim obciążeniem dla d = 15 m

4.1.2. Triple loading

Table 3

Deflection under the third load for v = 60 m/sec

Spacing [m]	Force model			Static deflection u_{stat} [m]
	u_{max} [mm]	x_{max}/L	u_{max}/u_{stat}	
9	5,04	0,380	1,309	3,85
12	3,32	0,357	1,099	3,02
15	2,64	0,540	0,992	2,66
18	3,12	0,530	1,328	2,35
21	2,89	0,462	1,431	2,02
24	2,03	0,348	1,140	1,78
27	2,16	0,710	1,213	1,78
30	3,65	0,666	2,051	1,78

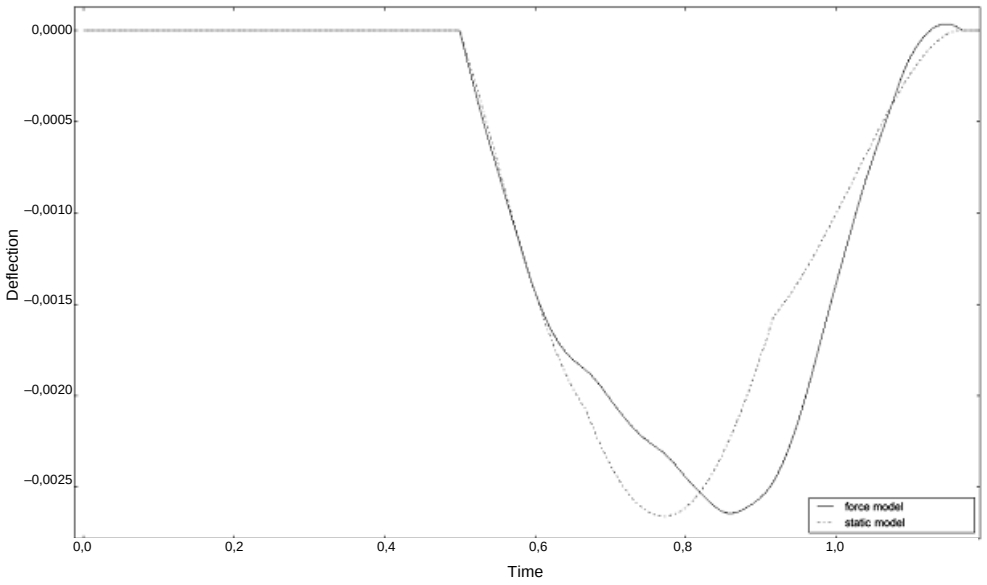

Fig. 5. An example of deflection of the beam under the third load by d = 15 m

Rys. 5. Przykład ugięcia belki w punkcie pod trzecim obciążeniem dla d = 15 m

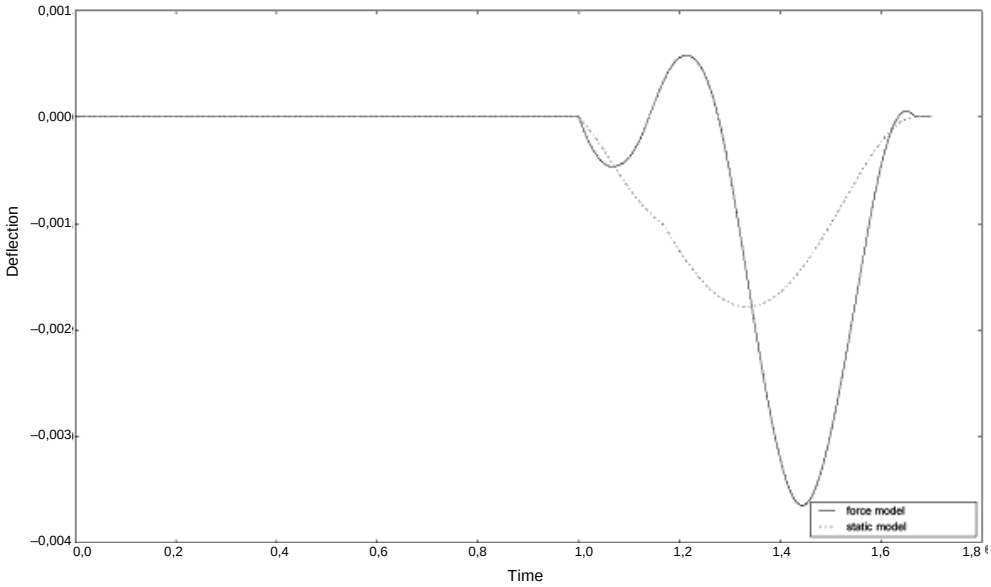

Fig. 6. An example of deflection of the beam under the third load by d = 30 m

Rys. 6. Przykład ugięcia belki w punkcie pod trzecim obciążeniem dla d = 30 m

4.2. Results for speed v = 70 m/sec

d_1 = 37.24 m d_{opt} = 18.62 m

4.2.1. Double loading

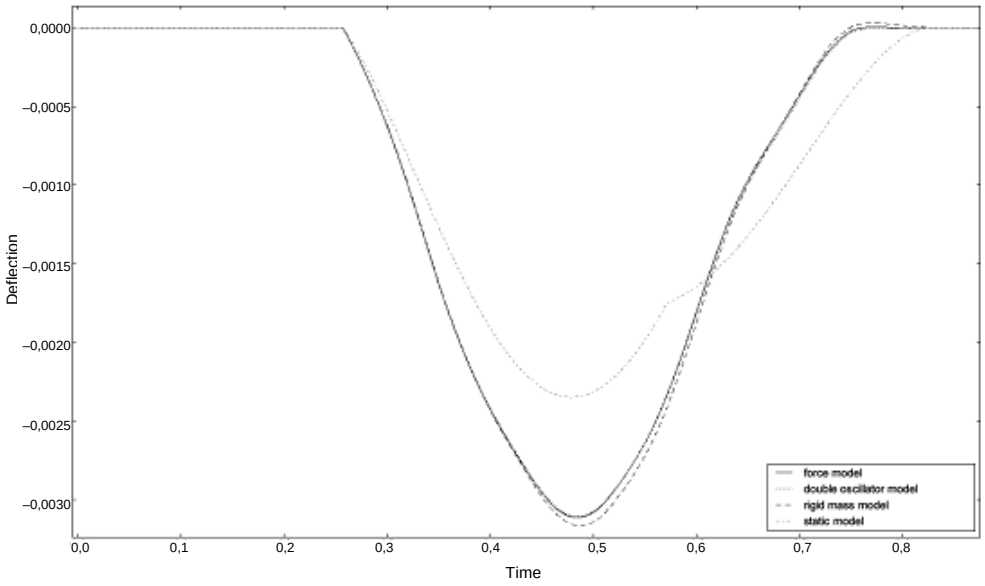

Fig. 7. An example of deflection of the beam under the second load by d = 18 m

Rys. 7. Przykład ugięcia belki w punkcie pod drugim obciążeniem dla d = 18 m

Table 4

Deflection under the second load for v = 70 m/sec

Spacing [m]	Force model			Oscillator model			Rigid mass model			Static deflection u_{stat} [m]
	u_{max} [mm]	x_{max}/L	$u_{max}/u_{st\ at}$	u_{max} [mm]	x_{max}/L	$u_{max}/u_{st\ at}$	u_{max} [mm]	x_{max}/L	$u_{max}/u_{st\ at}$	
9	5,25	0,515	1,646	5,20	0,515	1,630	5,30	0,524	1,661	3,19
12	4,64	0,475	1,578	4,61	0,475	1,568	4,70	0,482	1,599	2,94
15	3,91	0,441	1,470	3,90	0,442	1,466	3,97	0,449	1,492	2,66
18	3,11	0,399	1,323	3,10	0,399	1,319	3,16	0,406	1,345	2,35
21	2,28	0,347	1,129	2,28	0,348	1,129	2,32	0,348	1,149	2,02
24	1,55	0,254	0,871	1,55	0,258	0,871	1,58	0,252	0,888	1,78
27	1,96	0,744	1,101	1,95	0,744	1,096	1,92	0,746	1,079	1,78
30	2,70	0,715	1,517	2,67	0,715	1,500	2,67	0,722	1,500	1,78

4.2.2. Triple loading

Table 5

Deflection under the third load for v = 70 m/sec

Spacing [m]	Force model			Static deflection u_{stat} [m]
	u_{max} [mm]	x_{max}/L	u_{max}/u_{stat}	
9	5,96	0,420	1,548	3,85
12	3,98	0,354	1,318	3,02
15	2,24	0,291	0,842	2,66
18	2,67	0,582	1,136	2,35
21	3,25	0,537	1,609	2,02
24	3,04	0,440	1,708	1,78
27	2,26	0,328	1,270	1,78
30	1,72	0,803	0,966	1,78

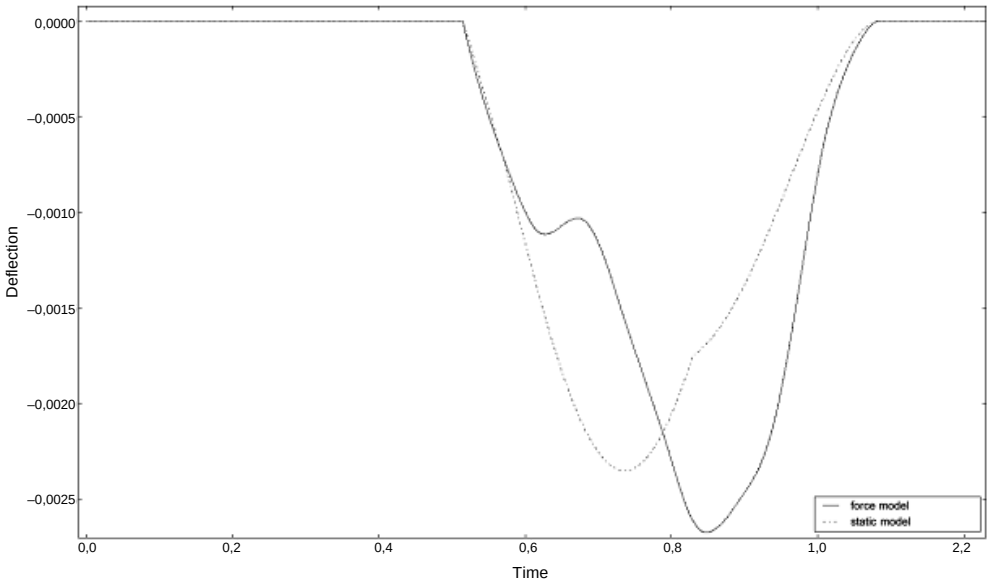

Fig. 8. An example of deflection of the beam under the third load by d = 18 m

Rys. 8. Przykład ugięcia belki w punkcie pod trzecim obciążeniem dla d = 18 m

Results proved correctness of above-mentioned assumptions of optimizing load spacing, and the correctness was as higher as more loads were applied. Results for analyzed models differ from each other, but difference is not significant. Finally this approach could be used

for designing bridge structures with minimizing dynamical effects of loading with high speed trains, after verification of this simulation with existing bridges measurements.

References

[1] Frýba L., *A rough assessment of railway bridges for high speed trains*, Engineering Structures 23, 2001, 548-556.
[2] Wang J.F., Lin C.C., Chen B.L., *Vibration suppression for high-speed railway bridges using tuned mass dampers*, International Journal of Solids and Structures 40, 2003, 465-491.
[3] Den Hartog J. P., *Drgania mechaniczne*, Warszawa 1971.
[4] Krylov V.V., *Noise and vibration from high-speed trains*, London 2001.
[5] Bogacz R., Bajer Cz., *Active control of beams under a moving load*, Journal of Theoretical and Applied Mechanics 3, 38, 2000.